Factors limiting the efficiency of molecular photovoltaic devices

Jenny Nelson,[1,*] James Kirkpatrick,[1] and P. Ravirajan[1,2]
[1]*Centre for Electronic Materials and Devices, Department of Physics, Imperial College London, London SW7 2BW, United Kingdom*
[2]*Department of Physics, University of Jaffna, Jaffna, Sri Lanka*
(Received 5 July 2003; revised manuscript received 17 September 2003; published 30 January 2004)

We present a simple model of a molecular photovoltaic device consisting of a two-level system, connected to external contacts by chains of one or more charge transporting orbitals. Electrons may be promoted in the two-level system by photon absorption, and charge transported to the external circuit by electron transfer between neighboring orbitals. Photon absorption and emission are described by a generalized Planck equation and electron transfer is described by nonadiabatic Marcus theory. We find the steady-state current by solving the set of coupled rate equations for electron transfer in the system under illumination as a function of bias applied to the contacts. We calculate monochromatic current-voltage characteristics and power conversion efficiency as a function of the system size, orbital energy levels, and electron transfer rates, and compare with the monochromatic detailed balance limit. Using realistic values of the energy levels and charge-transfer rates, we are able to reproduce a number of commonly observed features in the current-voltage characteristics. These include a ''kink'' in the current-voltage curve close to open circuit when large interfacial energy steps are present or mobilities are low, and a reduction of the open-circuit voltage and crossing of the light and dark current curves when interfacial recombination is strong. We show that open-circuit voltage is dominated by the acceptor-donor energy gap when recombination is important, and by the optical gap when recombination is low. We confirm previous reports that photovoltaic energy conversion can be achieved by interfacial asymmetry alone and that a potential difference between the electrodes is unnecessary. Improved photovoltaic efficiency of molecular heterojunctions requires ohmic contacts, improved charge-carrier mobilities, and tuning of the electron-transfer rates at the heterojunction. Maximizing the rate of charge separation does not necessarily lead to maximum efficiency.

DOI: 10.1103/PhysRevB.69.035337 PACS number(s): 73.40.Lq, 72.40.+w, 72.80.Le

I. INTRODUCTION

Molecular electronic materials such as dyes, conjugated polymers, and small molecules are gaining interest for applications in photovoltaics. Attractive features are the possibility of solution processing, compatibility with flexible substrates, and the low materials consumption for ultrathin molecular films, all of which offer the prospect of cheaper photovoltaic energy generation. Recent improvements in device design have led to power conversion efficiencies exceeding 3% in several distinct material systems.[1–3] All of these devices rely upon the dissociation of a photogenerated excitation at the interface between an electron donating and electron accepting material, in one case aided by a sensitizer.

Compared to inorganic solar cells, molecular photovoltaic devices are characterized by a relatively low photocurrent density and low fill factor. The low photocurrent density is attributed to the limited spectral sensitivity of molecular solids, and the poor fill factor to slow charge transport and high recombination. Improving these requires both the development of materials with superior properties (light absorption, mobility) and an understanding of the device physics of molecular solar cells.

Recent studies[4–9] have helped to elucidate the mechanism of photocurrent generation in molecular heterojunctions. In particular, it has been demonstrated that, unlike conventional *p-n* and *p-i-n* semiconductor structures, the photovoltage of a molecular heterojunction is *not* limited by the potential difference due to different contact work functions. In conventional devices photogeneration is distributed throughout the active layers and contributions to the photovoltage from concentration gradients are negligible, while in molecular heterojunctions strongly localized photogeneration leads to large and asymmetric gradients in charge-carrier density which are sufficient to generate a high photovoltage.[4,5]

Such developments have helped to elaborate a device physics for organic solar cells. However, the question of the limiting power conversion efficiency for a molecular solar cell has not yet been addressed. In crystalline semiconductor solar cells, a detailed balance treatment has been applied to calculate the limiting efficiency η under solar illumination. For a material with complete light absorption for photon energy E greater than some threshold E_g, complete charge separation, and infinite charge-carrier mobilities, η has a maximum of 31% at $E_g = 1.3$ eV (e.g., Ref. 10). Practical solar cells reach 25% (Ref. 11) and the reasons for the shortfall in efficiency are reasonably well understood (i.e., shading, series resistance, and surface recombination). The same limit cannot readily be applied to molecular photovoltaic systems, which are characterized by narrow spectral absorption, low mobilities, and require an additional intermolecular electron-transfer step to achieve charge separation. These features are due to the molecular nature of the materials and must be incorporated in any realistic model, and all three represent losses compared to the detailed balance limit. The first effect, the loss in photocurrent due to the narrow spectral sensitivity of molecular materials, is reasonably well understood. Indeed, new molecular photovoltaic device concepts are often evaluated in terms of their *monochromatic* power conversion efficiency. The remaining losses, due to

the rates of intermolecular charge transfer and transport, are still largely unquantified.

The purpose of this paper is to examine the loss mechanisms due to charge transfer, *independent* of those due to poor light absorption, by modeling the molecular photovoltaic device as a two-level system. We consider photon absorption and emission in terms of a detailed balance treatment and intermolecular charge transfer in terms of nonadiabatic Marcus theory. We will show that the monochromatic current-voltage characteristics and the maximum efficiency are functions of the relevant energy levels of the photovoltaic device, the intermolecular electron-transfer parameters and the light intensity. The simple model reproduces a number of features observed in experimental systems and predicted by more sophisticated models.

II. MODEL

The core of the model is a two-level system consisting of a lower energy level [the highest occupied molecular orbital (HOMO)], which is normally filled, separated by an energy gap of E_g from an upper level [the lowest unoccupied molecular orbital (LUMO)], which is normally empty. This represents the central light absorbing molecule or ''sensitizer.'' Photons of energy E_g can excite electrons from HOMO to LUMO producing an excited state (exciton). The excited state may decay by radiative relaxation of the electron to the HOMO (''intramolecular'' recombination). Alternatively, the promoted electron may be transferred to an adjoining ''acceptor'' orbital or directly to a charge collecting (n-type) contact, or the vacancy in the HOMO level may be filled by electron transfer from an adjoining ''donor'' orbital or directly from a second (p-type) contact. Each orbital is considered to have only two valence states, i.e., double ionization is assumed to be energetically unfavorable, and for the sensitizer, only the first neutral excited state is included. The system is assumed to be charge neutral in all conditions. Since observations are usually ensemble averages over a large number of similar systems in different states, it is valid to consider the occupation of states in terms of Fermi-Dirac occupation probabilities.

We consider the three systems illustrated in Fig. 1. In (a) the LUMO, at energy E_c, attaches directly to the n contact and the HOMO, at energy E_v, attaches to the p contact. In (b) and (c), contact is made via acceptor and donor orbitals at energies E_a and E_d, respectively. Physically, the acceptor and donor orbitals may belong to adjoining layers of other organic materials of larger optical gap, or the interfacial layer at a metal-organic contact. Remote orbitals of these adjoining molecules, such as the HOMO of the acceptor and the LUMO of the donor, are assumed to lie so far above or below the sensitizer orbitals that they are not involved in electron transfer. This is normally the case for experimental systems. In case (c) a chain of N additional acceptor orbitals connects the first acceptor level to the n contact and N additional donor levels connect the donor to the p contact. In all cases the transport of charge from final orbital to contact is lossless, i.e., the quasi-Fermi levels of that orbital and the neighboring contact are identical. The acceptor and donor

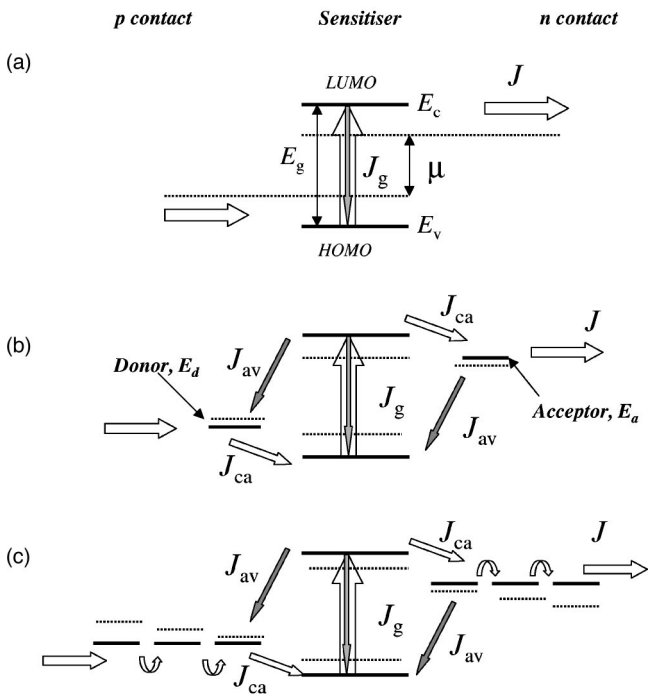

FIG. 1. Energy-level diagrams for the three systems discussed in the text. Unshaded arrows show forward electron-transfer pathways (generating photocurrent) while shaded arrows show recombination pathways (intramolecular and interfacial). Dotted lines represent the Fermi levels at short circuit. Other orbitals of the acceptor and donor molecules do not take part in electron transfer and are not shown.

energies are placed symmetrically about the center of the optical gap. Cases (b) and (c) may be considered crude models of a three-layer photoconverter such as a dye-sensitized solar cell.[1,12] Cases (a) represents the detailed-balance limit for monochromatic energy conversion. Comparing the characteristics of cases (b) and (c) with cases (a) reveals loss mechanisms due to intermolecular charge transfer. Though we focus on symmetric systems to simplify the analysis, the main features (effects of orbital energies, transfer rate, and chain length) can be extended to more general donor-acceptor and donor-sensitizer-acceptor heterojunctions.

A. Light absorption

The rates of absorption and spontaneous emission of photons of energy E_g by the two-level system can be described with Fermi's golden rule.[10] Applying detailed balance between absorption and emission in a photon flux leads to the following expression for the net steady-state transition rate R from HOMO to LUMO per unit volume:

$$R=\rho\left(G_s+G_a-\frac{K_g}{e^{(E_g-\mu_c+\mu_v)/kT}-1}\right)(f_v-f_c), \qquad (1)$$

where f_v and f_c are the occupation probabilities of the HOMO and LUMO, respectively, μ_v and μ_c their quasi-Fermi energies (defined through $f_i=[1+\exp((E_i-\mu_i)/kT)]^{-1}$), ρ is the volume density of identical two-level

systems, k is Boltzmann's constant, T the temperature and K_g a coefficient of recombination (defined below). G_s and G_a represent the rates of absorption of solar and ambient photons, given by $G_s = f_{osc} b_s$ and $G_a = f_{osc} b_a$, where f_{osc} is the oscillator strength of the sensitizer and b_s, b_a are the incident spectral photon flux densities from the sun and the ambient, respectively. f_{osc} is the relevant quantity defining absorption by a discrete level in a panchromatic spectrum, since it is bandwidth independent and ensures that the absorption is independent of the broadening of the molecular levels. Modeling the sun as a black body at temperature T_s we have for the solar and ambient flux densities

$$b_s = \frac{2\pi X F_s}{c^2 h^3} \frac{E^2}{(e^{E/kT_s} - 1)} \tag{2}$$

and

$$b_a = \frac{2\pi (1 - X F_s)}{c^2 h^3} \frac{E^2}{(e^{E/kT_a} - 1)}, \tag{3}$$

where F_s is the relative angular range of the sun, X the concentration factor, T_a the temperature of the ambient, h is Planck's constant, and c the speed of light. Both fluxes are evaluated at $E = E_g = E_c - E_v$. Ensuring detailed balance, K_g is then given by

$$K_g = f_{osc} (2\pi E_g^2 / h^3 c^2), \tag{4}$$

where we have used the three-dimensional density of photon states, $g_\gamma = 8\pi n^3 E^2 / h^3 c^3$, and resolved the emission in the forward direction, perpendicular to the plane of the device, assuming that emission occurs into free space (refractive index $n = 1$). Equation (1) is equivalent to the generalized Planck equation which has been used to describe radiative recombination in semiconductor based[13] and dye based[14] solar cells.

Assuming that all excitations which do not relax lead to charge separation, the current density generated by light absorption in the molecular assembly, J_g, is given by

$$J_g = q \int_0^d R dx, \tag{5}$$

where q is the electronic charge and the integral is taken over the thickness d of the device. (We choose the sign of J_g such that short circuit photocurrent is positive.) At this point we choose to focus on systems which are optically thin. Although in the usual detailed-balance treatment of solar cell efficiency unit absorptivity and uniform quasi-Fermi levels are assumed, this is physically unreasonable for low mobility systems. Therefore we consider a thin molecular assembly but calculate efficiency in terms of *absorbed* rather than *incident* photon flux, in order to make direct comparison with the detailed balance limit. This yields the net photogenerated current density

$$J_g = q\rho d \left(G_s + G_a - \frac{K_g}{e^{(E_g - \mu_c + \mu_v)/kT} - 1} \right) (f_v - f_c). \tag{6}$$

We recognize that this description of transitions in a two-level system is a very crude approximation to a real molecular sensitizer. Optical transitions in molecules are strongly influenced by vibronic and excitonic effects, while charge separation may also involve the formation of intermediate species such as bound polaron pairs. A more realistic model should include a more detailed description of the photogeneration and recombination pathways. However, we stress that the *qualitative* features predicted here will result for any mechanism where the probability of recombination increases with the population of occupied LUMO and unoccupied HOMO states.

B. Intermolecular electron transfer

For all intermolecular electron-transfer steps from an initial state i to a final state f, we use the rate expression from nonadiabatic Marcus theory,[15,16]

$$k_{i \to f} = C_{if} \lambda_{if}^{-1/2} e^{-(\Delta_{if} - \lambda_{if})^2 / 4\lambda_{if} kT} f_i (1 - f_f), \tag{7}$$

where C_{if} includes the wave-function overlap between initial and final states, including the Franck-Condon factor, Δ_{if} represents the free-energy difference between initial and final states, λ_{if} the reorganization energy, and f_i, f_f the Fermi-Dirac occupation factors for initial and final state. In what follows we neglect changes in Coulomb energy so that

$$\Delta_{if} = E_i - E_f. \tag{8}$$

The relevant electron-transfer pathways (i,f) are LUMO to acceptor, ca (which is equivalent to donor to HOMO in symmetric systems), acceptor to acceptor, aa (equivalent to donor to donor), and acceptor to HOMO, av (equivalent to LUMO to donor) (see Fig. 1). To obtain the net electron-transfer rate, and hence current, we add the forward rate $k_{i \to f}$ to the backward rate $k_{f \to i}$ for each pathway, respecting the sign of Δ_{if}. This gives for the current density

$$J_{if} = q\rho d K_{if} [f_i (1 - f_f) - e^{-\Delta_{if}/kT} f_f (1 - f_i)] \tag{9}$$

for each of the pathways ca, av, where

$$K_{if} = C_{if} \lambda_{if}^{-1/2} e^{-(\Delta_{if} - \lambda_{if})^2 / 4\lambda_{if} kT}. \tag{10}$$

For electron transfer between the $(n-1)$th and nth orbitals in the acceptor chain, we have the current density

$$J_{aa}^n = q\rho d K_{aa} [f_a^{n-1} (1 - f_a^n) - e^{-\Delta_{aa}/kT} f_a^n (1 - f_a^{n-1})], \tag{11}$$

where

$$K_{aa}(V) = C_{aa} \lambda_{aa}^{-1/2} e^{-(\Delta_{aa} - \lambda_{aa})^2 / 4\lambda_{aa} kT}, \tag{12}$$

where f_a^{n-1} and f_a^n refer to the occupation probabilities and Δ_{aa} to the free-energy difference between adjacent orbitals. Orbitals are numbered from 0 (adjacent to sensitizer) to N (adjacent to electrode). For isoenergetic acceptors as considered here, $\Delta_{aa} = -q(\phi_{n-1} - \phi_n)$, where ϕ_n is the electrostatic potential at the nth orbital. K_{aa} is therefore a function

of the applied bias V, and is shown as such in Eq. (12). We shall see below that when the device is developing a voltage, Δ_{aa} is negative.

C. Calculation of current-voltage characteristics

To solve for the current-voltage characteristic of each of the structures in Fig. 1, we calculate the net electron current J passing from the p to n electrode as a function of the difference in quasi-Fermi level of the orbitals attached to those electrodes. (Note that J is defined such that short circuit photocurrent is positive.) In each case the Fermi level is constant at a level, $\mu_0 = E_v + E_g/2$, in equilibrium.

Steady state ensures that the net current at each orbital is zero. Therefore for case (a) we have $J = J_g$ and $qV = \mu_c - \mu_v$. This reduces to $qV = 2(\mu_c - \mu_0)$, exploiting the symmetry of the system.

For case (b), we have the joint constraints $J = J_{ca} - J_{av}$ and $J_g = J_{ca} + J_{av}$ with $qV = \mu_a - \mu_d = 2(\mu_a - \mu_0)$, where μ_a, μ_d are the quasi-Fermi levels of acceptor and donor level. In the case of no interfacial recombination ($K_{av} = 0$), the current density for case (b) simplifies to $J = J_{ca} = J_g$.

For case (c), where interfacial recombination is not considered, we have in addition $J = J_{aa}^n$ for $n = 1,\ldots,N$, with

$$qV = 2(\mu_a^N - \mu_0), \tag{13}$$

where μ_a^n is the quasi-Fermi level of the nth acceptor orbital in the chain.

Cases (a) and (b) are solved exactly, and (c) is solved numerically.

As explained above, we have chosen to deal with systems which are optically thin in order to make direct comparison with the detailed balance limit. In this case the most useful quantity is the internal quantum efficiency (IQE)

$$I = J/q\rho d G_s \tag{14}$$

and we define the power conversion efficiency in terms of absorbed rather than incident photon flux, i.e., by the maximum value of

$$\eta = \frac{qIV}{E_g} = \frac{JV}{\rho d G_s E_g} \tag{15}$$

in the range $0 < V < V_{oc}$, where V_{oc} is the open-circuit voltage. (The power conversion efficiency incorporating absorptivity is recovered by multiplying η by the fraction of light absorbed.)

D. Solutions for *I-V*

Explicit solutions for I-V are found in cases (a) and (b), by exploiting the symmetry of the system. The detailed balance solution [case (a)] is given by the parametric equations

$$I = \frac{1}{G_s}\left(G_s + G_0 - \frac{K_g}{x_c^2 - 1}\right)\left(\frac{x_c - 1}{x_c + 1}\right) \tag{16}$$

and

$$qV = 2(\mu_c - \mu_0) = E_g - 2kT \ln x_c, \tag{17}$$

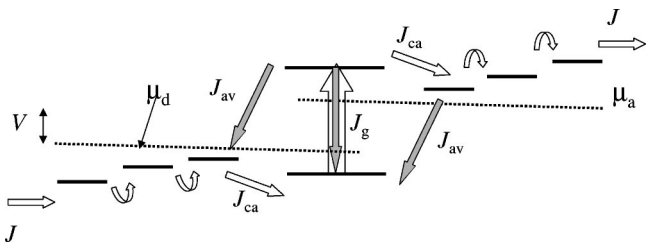

FIG. 2. Energy-level diagram and chemical potential for case (c) at operating condition. The gradients in electron and ''hole'' quasi-Fermi levels, μ_a and μ_d (dotted lines), indicate the direction of electron flow. The photogenerated potential difference between n and p contacts biases the system to oppose photocurrent generation.

where

$$x_c = \exp[(E_c - \mu_c)/kT]. \tag{18}$$

The open-circuit voltage V_{oc} is given by

$$V_{oc} = E_g - kT \ln\left(\frac{K_g}{G_s + G_0} + 1\right). \tag{19}$$

In case (b), a larger set of equations (see Appendix) gives I and V as functions of x_c, and V_{oc} is found implicitly as the point where $I = 0$. In the limit of no interfacial recombination, case (b) simplifies to a form similar to Eq. (16) and V_{oc} is again given by Eq. (19).

In case (c), where chains of acceptors and donors are present, the system is complicated by the V dependence of intermolecular transfer along the chains and cannot be solved explicitly. We make the assumption that the applied bias is divided equally between the intervals connecting neighboring donors and acceptors in the chains, so that the intermolecular energy difference is

$$\Delta_{aa} = -V/2N \tag{20}$$

for all neighboring donors or acceptors. The intermolecular electron transfer rate, Eq. (12), is thus a function of V,

$$K_{aa}(V) = C_{aa}\lambda_{aa}^{-1/2} e^{-(V/2N + \lambda_{aa})^2/4\lambda_{aa}kT}. \tag{21}$$

Note that the sign of Δ_{aa} is negative for positive applied bias. This is expected for a system with similar electrode work functions where there is no built-in bias in equilibrium (as shown in Refs. 4,5). When the device generates photocurrent, electrons flow from the p to the n electrode, establishing a potential difference which opposes further electron flow.

Figure 2 illustrates the orbital energies and quasi-Fermi levels of system (c) in the general operating condition. At short circuit, $\Delta_{aa} = 0$ and the current is driven by the gradient in quasi-Fermi levels, which is then at its maximum value. At open circuit, μ_a and μ_d are constant for all acceptors or donors and Δ_{aa} has its maximum magnitude within the photovoltaic regime.

We solve case (c) by first solving the central donor-sensitizer-acceptor unit explicitly [as case (b)] for J and μ_a^0. Then, for each J, the value of V is found which satisfies

$J_{aa}=J$ using Eqs. (11), (20), and (21). Compared to case (b), the effect of adding the chains is to decrease the value of V for positive J points and to increase V for negative J points, similar to the effect of adding a series resistance.

In all cases, the dark J-V characteristic is calculated exactly as the light curve but with $X=0$ in Eqs. (2) and (3).

III. RESULTS

A. Values of parameters used

We have tried to use parameter values typical of real molecular photovoltaic systems, as far as these are known. We focus on a system with band gap $E_g=2$ eV since this is typical of the optical gap of commonly used organic electronic materials, and oscillator strength f_{osc} of 1×10^{-21} eV m^2. This value of f_{osc} is typical of a simple light absorbing polymer and is equivalent to a decadic extinction coefficient of 10 000 dm^3 mol^{-1} cm^{-1} over a bandwidth of about 0.5 eV centerd on E_g. It corresponds to the order of one excitation per molecule per second at one-sun solar illumination. For the forward electron-transfer rate K_{ca} we consider a wide range of values from 10^2 to 10^{15} s^{-1}. A value of around 10^{12} s^{-1} compares well with subpicosecond transfer rates reported for polymer-fullerene[17,18] and dye-sensitized[19] photovoltaic systems. K_{ca} represents the maximum electron-transfer rate, i.e., it is assumed that $\lambda_{ca}=E_{ca}$. For the acceptor and donor levels we consider values which are within a few tenths of an eV of the LUMO and HOMO, respectively. Values of Δ_{ca} for experimental systems range from around 0.3 eV for the LUMO-TiO_2 gap in dye-sensitized systems,[20] to 0.5–1 eV for polymer blend systems,[21,22] to around 0.9 eV for polymer-fullerene systems,[24] and over 1 eV for polymer-metal oxide systems.[23] When interfacial recombination is present, we assume that C_{av} is equal to the coefficient C_{ca} for forward transfer and select the back electron-transfer rates K_{av} by choosing the reorganization energy λ_{av}. λ_{av} is varied from a few tenths of an eV to over 1 eV, modulating K_{av} by ten orders of magnitude. Although not well known, reorganization energies for back electron transfer are expected to be relatively large, of order 1 eV, consistent with slow transfer.[25] For intermolecular electron transfer along chains, we consider low-field rates $K_{aa}(0)$ in the range 10^4–10^{12} s^{-1}. This incorporates the relevant range of organic charge-carrier mobilities [see Eq. (22) below]. Chain lengths from 1 to over 100 nm are considered.

For the light source we have used a black body sun of temperature $T_s=5760$ K and angular range $F_s=2.16\times10^{-5}$ at one-sun concentration.[10] The ambient (and cell) temperature is taken as $T=300$ K. These fix the intramolecular (i.e., radiative) recombination rate, as a function of the HOMO and LUMO occupation levels. In most cases below, we present the results as I-V rather than J–V plots, to avoid dependence on the system thickness. For comparison with light I-V curves, dark currents are divided by the factor $q\rho dG_s$ for the relevant light intensity.

B. Effects on the I-V characteristic

1. Detailed-balance limit

In the monochromatic detailed-balance limit [case (a)] the internal quantum efficiency at short circuit is always unity by definition, and the I-V curve is a function only of the energy gap and concentration X. The monochromatic power conversion efficiency increases monotonically with band gap and with light intensity. For our standard case with $E_g=2$ eV and $f_{osc}=10^{-21}$ eV m^2, η varies with concentration from 0.73 at one sun to over 0.8 at maximum concentration, as shown in Fig. 3. The I-V curve for this system at one sun is shown in Fig. 4.

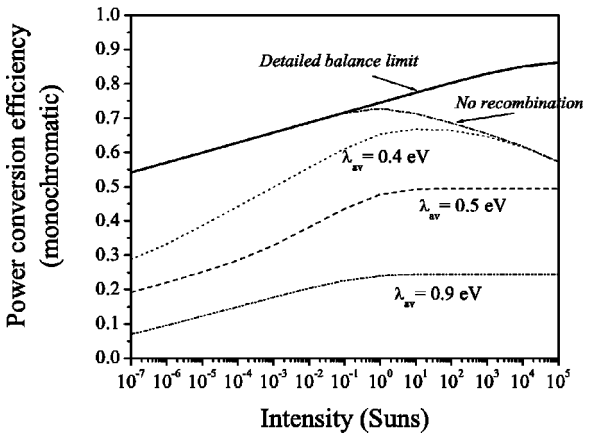

FIG. 3. Monochromatic power conversion efficiency (assuming unit absorptivity) of a two-level system with optical gap of 2 eV and oscillator strength 1×10^{-21} eV m^2 as a function of light intensity under a 5760-K black body sun. The full line shows the detailed-balance limit. Broken lines show the system in case (b) with $\Delta_{ca}=0.7$ eV, $K_{ca}=10^{12}$ s^{-1}, and different electron-transfer rates for interfacial recombination, characterized by different reorganization energies. $\lambda_{av}=0.4$ eV, 0.5 eV, and 0.9 eV correspond to electron-transfer rates K_{av} of 4.2×10^3 s^{-1}, 5.0×10^6 s^{-1}, and 1.6×10^{11} s^{-1} respectively.

2. Effect of donor and acceptor orbitals

For the system with donor and acceptor orbitals [case (b)] we first consider the case when recombination is absent ($K_{av}=0$) and look at the effect of independently varying the forward electron-transfer rate K_{ca} and the interfacial energy step Δ_{ca}. I-V curves at one sun for the systems with $\Delta_{ca}=\lambda_{ca}=0.3$ eV and $\Delta_{ca}=\lambda_{ca}=0.7$ eV, for a range of K_{ca}, are shown in Figs. 4(a) and 4(b). In each case, the I-V curve tends to the detailed-balance limit for sufficiently high K_{ca}. As K_{ca} is reduced, the I-V curve degrades, developing a point of inflection, or ''kink,'' near open circuit. The I-V curve then recedes, so that the current falls off at a voltage lower than V_{oc} (the ''fall-off'' voltage) and the maximum power point moves to lower voltages. When the fall-off voltage reaches a limiting value close to $(E_a-E_d)/q$, the curve stops receding and the photocurrent begins to reduce in magnitude. For larger Δ_{ca}, the effect of reducing K_{ca} is more pronounced and this limiting voltage is lower. As the I-V curve degrades, the negative I part of the I-V curve and the dark current are both suppressed in magnitude.

The behavior may be understood by considering Eq. (9) for J_{ca} as voltage (and hence μ_a) increases and f_a approaches unity. For finite electron-transfer rate K_{ca} a difference in quasi-Fermi levels, $\mu_c>\mu_a$, is then required to drive

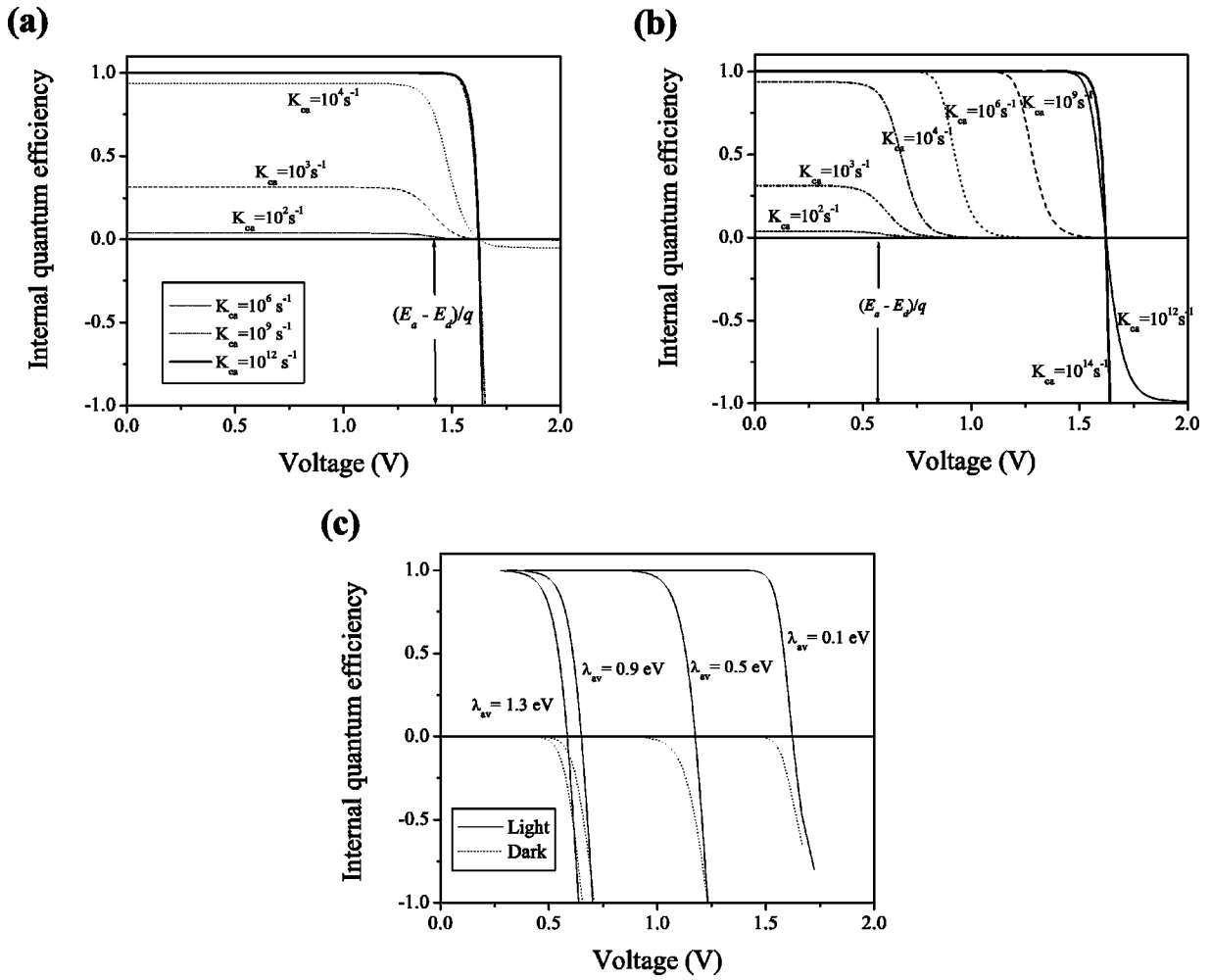

FIG. 4. Internal quantum efficiency–voltage (I-V) curves for the system in case (b) with optical gap of 2 eV and oscillator strength 2×10^{-21} eV m^2 under a 5760-K black body sun. (a) $\Delta_{ca}=0.3$ eV and $K_{av}=0$ for different values of K_{ca}. (b) $\Delta_{ca}=0.7$ eV and $K_{av}=0$ for different values of K_{ca}. (c) $\Delta_{ca}=0.7$ eV and $K_{ca}=10^{12}$ s^{-1} for different interfacial recombination rates. ($\lambda_{av}=0.1$ eV, 0.5 eV, 0.9 eV, and 1.3 eV correspond to electron-transfer rates K_{av} of 10^{-49} s^{-1}, 5.0×10^6 s^{-1}, 1.6×10^{11} s^{-1}, and 7.3×10^{11} s^{-1}, respectively.) In (a) and (b), note that the degradation of the I-V curve near V_{oc} occurs more easily for the larger interfacial energy step, and that the magnitude of the IQE collapses at a voltage close to $(E_a-E_d)/q$. The effect of interfacial recombination (c) is to reduce the open-circuit voltage and to increase the limiting reverse current. Although dark current is also increased, the light and dark currents now cross. V_{oc} is linked to E_g under weak recombination and $(E_a-E_d)/q$ under strong recombination.

electrons from LUMO to acceptor. This means that μ_c reaches the value where intramolecular recombination becomes important, and which determines the open-circuit condition in the detailed-balance case, before μ_a reaches this value. As V is further increased, μ_c remains pinned at its open-circuit value until μ_a equals it to bring the system into the true open-circuit condition. In this regime intramolecular recombination competes with charge separation, and both J_g and J_{ca} fall towards zero. This kink effect is more pronounced for larger Δ_{ca} or lower K_{ca}, and for higher light intensity, leading to a decrease in power conversion efficiency with increasing X (shown in Fig. 3 for the case $\Delta_{ca}=0.7$ eV). Beyond open circuit, μ_a continues to rise until $f_a=1$ and J reaches its limiting value of $-e^{-\Delta_{ca}/kT}q\rho dK_{ca}$. This value is also the limit of the dark current, and is due to the limited rate of electron transfer between acceptor and LUMO.

These effects on the shape of the I-V curve are therefore a consequence of limited electron-transfer rates and limited density of states. With infinite K_{ca} (equivalent to the infinite mobility assumed in detailed balance), or with high density of acceptor states (preventing f_a from reaching 1), the I-V curve would be limited only by the rate of intramolecular recombination at the sensitizer, no kink would appear, and the negative current would never saturate with increasing V. One simple consequence of this behavior is that, in contrast to inorganic semiconductor devices, a low dark current does not necessarily lead to efficient photovoltaic energy conversion.

3. Effect of interfacial recombination

The effect of introducing *interfacial* recombination is shown in Fig. 4(c). This shows light and dark I-V curves for the system [as in Fig. 4(b)] with $\Delta_{ca}=0.7$ eV and K_{ca}

$=10^{12}$ s^{-1}, with different values of K_{av}. C_{av} is assumed equal to C_{ca} since the two electron-transfer pathways are between the same two molecules, and K_{av} is varied by varying λ_{av}. Figure 4(c) shows that as λ_{av} is increased from a small value towards Δ_{av}, where K_{av} is maximized, the open-circuit voltage decreases. The effect on V_{oc} is quite substantial. For λ_{av} values of 0.5–0.9 eV, V_{oc} decreases by between 0.5 and 1 V. Those values of λ_{av} are reasonable limits to the reorganization energy for the acceptor-dye recombination step in a dye-sensitized system.[25] The reduction in V_{oc} is larger for larger Δ_{ca} with the result that V_{oc} is linked to $E_a - E_d$ rather than to E_g, as it was in the detailed-balance limit. It is readily shown that when $E_a = E_d$ and $K_{ca} = K_{av}$, both photovoltage and photocurrent vanish, i.e., the photovoltaic effect depends upon asymmetry in the electron-transfer rates at the interface.

Introducing the new pathway allows ''cycling'' of electrons (HOMO-LUMO, LUMO-acceptor, acceptor-HOMO) so that the LUMO-acceptor current is no longer required to vanish at open circuit. Now as V is increased, the acceptor-HOMO current J_{av} increases and cancels out the photocurrent long before intramolecular recombination becomes significant. Open circuit is thus reached when μ_c is much smaller than its detailed-balance open-circuit value and the kink observed in Figs. 4(a) and 4(b), which is due to limited LUMO-acceptor transfer, disappears.

The additional recombination pathway also increases the saturation value of both the light current and the dark current. The effect is greater for the light current leading to a crossing of the light and dark currents below the V axis. Such crossings are commonly observed in molecular photovoltaic systems.[1,3,26,27] These different saturation currents in light and dark are due to the different magnitude of the limiting J_{av}. In the light, the occupation level of the HOMO ($=1-f_c$) is generally smaller than that in the dark, and consequently the limiting value of J_{av} is larger. Physically, we may consider that the photoionized sensitizers introduce an additional pathway for recombination in the light. Such an effect has been observed in dye-sensitized solar cells with polymer electrolyte, where the recombination current under illumination is observed to increase with increasing light intensity.[28]

In this system, increasing light intensity increases the efficiency of charge separation relative to interfacial recombination. Increasing X thus moves the system from a recombination limited regime at low X, through an optimum condition, to a charge-transfer-limited regime at high X. The effect on power conversion efficiency is illustrated in Fig. 3 for the systems in Fig. 4(c) with different K_{av}. V_{oc} increases with X in the recombination limited regime, before saturating in the transport limited regime. Such behavior has been observed experimentally.[5] Figure 3 shows that the power conversion efficiency can easily be reduced to one-quarter of the maximum available by interfacial recombination. These effects are studied in more detail in Ref. 29. (Note that because we are dealing with noninteracting molecular systems, we do not observe effects—typically the fall in efficiency with light intensity—which are due to bimolecular recombination.)

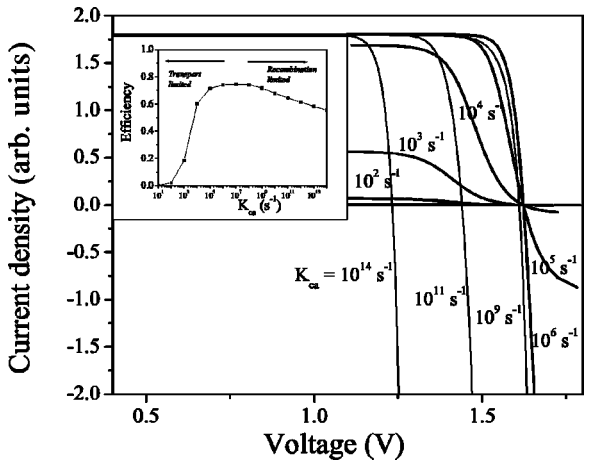

FIG. 5. Internal quantum efficiency curves for the system in Fig. 4(a) ($\Delta_{ca}=0.3$ eV) with $\lambda_{av}=0.7$ eV ($K_{av}\approx 7\times 10^9$ s^{-1}) and varying K_{ca}. Charge separation and interfacial recombination rates are linked through $C_{ca}=C_{av}$. Bold curves show the transport limited regime, where K_{ca} is less than the optimum ($K_{ca}<10^7$ s^{-1}), while light curves show the recombination limited regime where K_{ca} is too high ($K_{ca}>10^9$ s^{-1}). The inset shows the monochromatic power conversion efficiency as a function of K_{ca}.

4. Optimization of electron-transfer rate

The above discussion has identified two regimes, one where K_{ca} is low and intramolecular recombination dominates, and the other where K_{av} is significant and interfacial recombination dominates. K_{ca} and K_{av} are determined by the same parameter C_{ca} ($=C_{av}$) which suggests that simply by varying the intermolecular coupling factor C_{ca} we may move from one regime to the other. In Fig. 5 we show the resulting I-V curves, parametric in K_{ca}, for the case with $\Delta_{ca}=0.3$ eV and $\lambda_{av}=0.7$ eV. This clearly shows a transition from charge-transfer-limited behavior, characterized by a kink and low fill factor, at low K_{ca} through a maximum, to interfacial recombination limited behavior, characterized by low V_{oc}, at high K_{ca}. The behavior in the low K_{ca} regime is also produced for low intrachain mobility, and so it may more generally be considered a transport limited regime. This clearly demonstrates that the fastest charge separation rate does not necessarily lead to the highest efficiency.

5. Effect of chains of donors and acceptors

When the system is extended by adding chains of donors and acceptors, with zero-field intermolecular hopping coefficient $K_{aa}(0)$, the I-V curve degrades both with increasing chain length N and with decreasing $K_{aa}(0)$. The effect of varying $K_{aa}(0)$ for $N=10$ is illustrated in Fig. 6, for the system with $\Delta_{ca}=0.3$ eV and $K_{ca}=10^{12}$ s^{-1} and $K_{av}=0$. A reorganization energy λ_{aa} of 0.9 eV is used as typical for hole transport in organic semiconductors,[30] but other values lead to similar results, changing only the slope of the J-V curve near V_{oc}. Reducing $K_{aa}(0)$ introduces a kink in the J-V curve and suppresses the large V saturation current, exactly as reducing K_{ca} in Fig. 4. The explanation is analogous. In this case reducing $K_{aa}(0)$ (rather than K_{ca}) limits the rate of supply of charge from sensitizer to contacts, introduces a

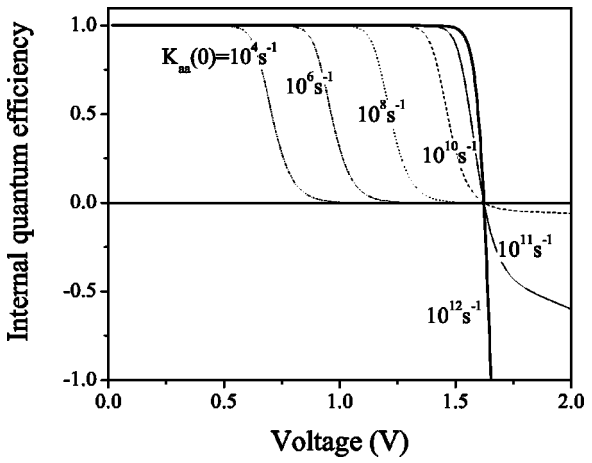

FIG. 6. *I-V* curves for the system in Fig. 4(a) ($\Delta_{ca}=0.3$ eV) with $K_{ca}=10^{12}$ s^{-1} and with ten additional acceptor and ten additional donor levels, as a function of $K_{aa}(0)$ [case (c)]. The effect of low mobility along the chains is to degrade the *I-V* curve, similar to the effect of decreasing K_{ca}. Increasing N produces a qualitatively similar effect to reducing $K_{aa}(0)$.

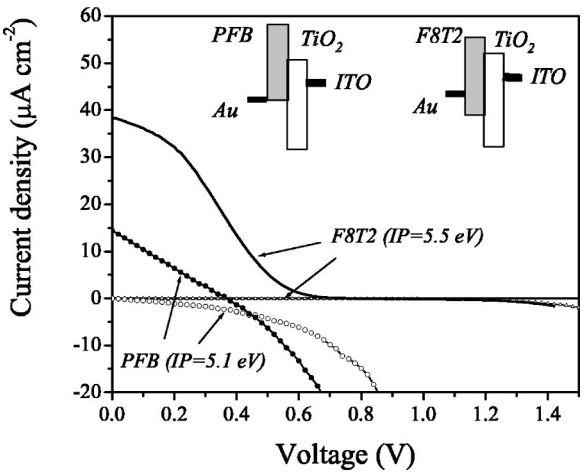

FIG. 7. Measured monochromatic light and dark current density-voltage curves for TiO_2/conjugated polymer/Au photovoltaic devices, made from polymers with different ionization potential (IP): F8T2 polymer, IP=5.5 eV and PFB polymer, IP=5.1 eV (Ref. 33). The effect of increasing the energy step between HOMO and cathode work function (nominally 5.1 eV for Au) is to degrade the *I-V* curve, as predicted in Fig. 4. (The low photocurrent for PFB polymer is due to weaker light absorption at the measurement wavelength.)

Fermi-level gradient between μ_c and μ_{a0}, and effective charge separation is stopped before true open circuit, as soon as intramolecular recombination begins. $K_{aa}(0)$ can be directly related to the low-field mobility ζ of the molecular chain, through

$$K_{aa}(0)=kT\zeta/qa^2, \tag{22}$$

where a is the intermolecular separation. A typical organic hole mobility of 10^{-4} cm^2 V^{-1} s^{-1} with $a=1$ nm leads to K_{aa} of order 10^8 s^{-1}. Figure 5 shows that such values may lead to degraded *I-V* curves in films only ten molecular spacings thick.

The effect of increasing N is similar to reducing $K_{aa}(0)$, and an example is presented below in Fig. 8. Both may be considered as a series resistance effect, also visible in the effect of the chain resistance on the gradient in $\partial J/\partial V$ close to V_{oc}. We show below that quantitatively and qualitatively similar behavior to Fig. 8(b) has been observed in practice. The effect of interfacial recombination on this system is again to reduce V_{oc}, as for the case without chains. Performance is then transport limited at low mobility, but becomes recombination limited and mobility independent at higher ζ values. The shape of the *J-V* curve is thus controlled by the relative importance of interfacial recombination and intermolecular charge transfer from sensitizer to electrodes.

6. Extension to donor-acceptor systems

So far we have considered donor-sensitizer-acceptor systems where only the central sensitizer absorbs light. This is most relevant to dye-sensitized solar cells but not obviously appropriate for other donor-acceptor photovoltaic systems. To address the wider validity of the model, we have solved two alternative systems, representing donor-acceptor systems. Both produce the same qualitative dependence of *I-V* characteristic on charge separation rate, recombination rate, and light intensity. The first model consists of equal chains of donors and acceptors joined at an interface, where only the donor and acceptor closest to the interface absorb light. The other is an asymmetric version of case (b) where $\Delta_{dv}=0$, and the sensitizer is assumed to be part of the donor phase. This may represent a bulk heterojunction solar cell[3,24] where light is absorbed in the donor and charge separation occurs only for excitons adjacent to the interface. Comparison of the *I-V* characteristics of this system with case (b) above shows that for systems where interfacial recombination is important, replacing the donor-sensitizer-acceptor system with the donor-acceptor system tends to increase V_{oc}. However, low mobility within the donor phase (represented by low K_{dv}) reduces the efficiency of charge separation and may tend to decrease photocurrent.

IV. DISCUSSION

A. Comparison with experimental systems

Several of the features discussed above for the simple model have been observed in experimental molecular photovoltaic systems. The kink in the *I-V* curves shown in Figs. 4–6 has been observed in devices made from multilayer, vacuum deposited molecular films[2,31,32] and in hybrid metal-oxide-polymer devices.[23,33] In all cases the kink is present when the energy step Δ at one or other collecting electrode exceeds about 0.4 eV. Reference 2 shows that replacing the indium tin oxide (ITO)-copper phthalocyanine (CuPc) interface ($\Delta=0.4$ eV) in a CuPc/C_{60} device with polyethylenedioxythiophene (PEDOT)-CuPc ($\Delta=-0.1$ eV) removes the kink in the *J-V* curve and improves device performance. A similar effect has been observed in the same system by modifying the electron collecting interface.[32] Recent studies in our laboratory of the effect of interfacial driving force on this

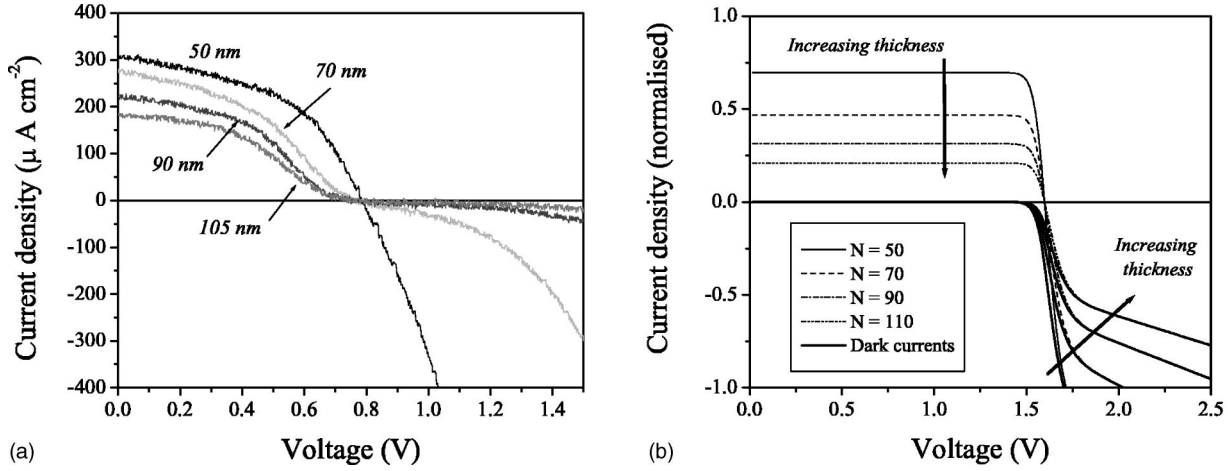

FIG. 8. (a) Measured current density-voltage curves for TiO_2/F8T2 polymer/Au devices with different polymer thicknesses under simulated sunlight (from Ref. 33). (b) Simulation of current density-voltage curves for the model [case (c)] for different lengths N of chains of acceptors and donors, representing different thicknesses, and allowing for optical filtering (see text). The qualitative behavior observed in (a) is reproduced. The experimental curves also show shunt resistance effects, not included in the model.

feature in TiO_2-polymer structures show that while the kink is present when Au (effective work function $\phi_w \simeq 4.9$ eV for Au on polymer) is deposited on poly(9,9-dioctylfluorene-Co-bithiophene) polymer (F8T2) polymer (ionization potential IP$=5.5$ eV), it is removed *either* by replacing the polymer with another of lower IP (of around 5 eV) or by replacing the Au with a contact of higher ϕ_w such as Pt (IP$\simeq 5.6$ eV) or PEDOT (IP$\simeq 5.3$ eV).[33] The effect is illustrated in Fig. 7. Note that reducing the interfacial step also results in a higher dark current, as expected from the model. The fact that the degradation of the J-V curve is observed for organic—metal interfaces suggests that only a limited density of sites at the metal interface is available for charge transfer with the organic layer.

Studies of the TiO_2-F8T2 polymer system show that the kink is more pronounced for higher light intensity[34] and for thicker polymer films.[33] Both are consistent with the model predictions in a general way. J-V curves as a function of polymer film thickness are reproduced from Ref. 33 in Fig. 8(a). The decreasing short circuit current density with film thickness is due to filtering of the incident photon flux by the ''dead'' layer of polymer lying more than one exciton diffusion length from the TiO_2 interface. In Fig. 8(b) we present simulated J-V curves as a function of thickness for the system in Fig. 4(b) ($E_a = 1.7$ eV) with chains of acceptors and donors 50–110 units in length. This system is not an ideal model for the experimental system since the model supposes an interface next to the sensitizer and a chain of hole transporting molecules leading from interface to p contact, while in the experimental system the chain occurs between the sensitizer and the interfacial step to the contact. Nevertheless, the effects of interface and chain are similar (both introduce a Fermi-level gradient between electrode and sensitizer) and by choosing conditions where the interfacial step is not limiting, we focus on the effect of chain length. For this system we calculate J rather than I to allow for the optical filtering effect. We use an absorption coefficient of 2×10^5 cm^{-1} and an exciton diffusion length of 5 nm, in accordance with experimental measurements,[33] an intermolecular spacing a of 1 nm and a relatively high mobility [$K_{aa}(0) = 10^{12}$ s^{-1}] in order to focus on chain length. Figure 8 shows that the behavior predicted by the model is very similar to that observed.

A further prediction of the model is that the effect of interfacial energy step on the J-V curve should be enhanced as temperature is reduced. This has in fact been observed in polymer/fullerene photovoltaic devices where the fill factor increases[35] and the J-V curve develops a point of inflection near V_{oc} (Ref. 36) as the measurement temperature is reduced from 50 °C to 20 °C.

In most experimental molecular photovoltaic systems, no kink is observed and V_{oc} is low compared to E_g/q. This suggests that interfacial recombination limits performance. In fact, the crossing of light and dark J-V curves in the negative J regime, which is shown in Fig. 4(c) to result from interfacial recombination, is commonly observed in practice.[1,3,26,27] The crossing effect is less severe in the systems which exhibit the best power conversion efficiency[1,3] indicating that interfacial recombination in those systems is slower. Relatively slow interfacial recombination in those systems (100 μs–1 ms) has indeed been confirmed by measurements.[37,38]

Finally, the model predicts that increasing driving force for charge separation should tend to improve J_{sc} and reduce V_{oc}. This is compatible with experimental studies of (liquid electrolyte) dye-sensitized solar cells, showing that increasing the electron affinity of the electron acceptor by coating with silica[39] or intercalation of lithium[40] leads to increased J_{sc} and reduced V_{oc} as expected. A study of the effect of varying the donor-HOMO energy step in solid-state dye-sensitized systems also showed that the yield of charge separation increases with increasing donor-HOMO driving force.[41]

B. Implications for device design

Although extremely simple compared to real devices, the model allows us to make some general comments about the design of molecular solar cells.

First, we have confirmed that photovoltage generation from a molecular heterojunction does not require any difference in work function of contact materials. In accordance with previous results,[4,5] our calculations show that photocarrier generation localized at a molecular heterojunction leads to photovoltages of order 1 eV, using typical physical parameters.

Second, we show that efficiency is a nontrivial function of the interfacial charge-transfer kinetics. Very fast interfacial charge transfer at the heterojunction leads to losses to interfacial recombination, and eventually to reduced efficiency. However, very slow charge transfer at heterojunction or other interfaces ultimately leads to intramolecular recombination and reduced efficiency. The latter factor means that contacts which are blocking for charge injection lead to poor photovoltaic performance. This implies that, in contrast to inorganic devices, the best efficiency is not achieved in devices with the lowest dark current.

For devices of order tens of nanometer thick, efficiency may be limited by the rate of intermolecular charge transfer through electron and hole transporting layers. Low charge-carrier mobilities lead to substantial Fermi-level gradients within the device, which enhance both intramolecular and interfacial recombination in the active region. Charge-carrier mobilities may need to be improved by 2–3 orders of magnitude to achieve reasonable efficiencies and optical depths. Poor mobility is also likely to enhance bimolecular recombination, which is not considered here.

In the most efficient experimental systems, interfacial recombination dominates V_{oc}. Monochromatic power conversion efficiencies in efficient molecular solar cells are around 10%.[42] Comparison of the parameters of the real photovoltaic system with our model shows that the primary loss is in V_{oc}, which is linked to the difference in the donor HOMO and acceptor LUMO levels and is much smaller than the optical gap. (Part of the difference is, however, due to the panchromaticity of the experimental systems, and other factors listed below.) Therefore to improve efficiency for any given system it is necessary to minimize the rate of interfacial recombination relative to the rate of charge separation. This may be achieved by tuning the energy steps, reorganization energies, or the intermolecular coupling. The interfacial charge-transfer kinetics may need to be *slowed down* to increase efficiency. Such an effect has indeed been observed in experimental dye-sensitized systems.[43]

To extend the analysis presented here to real molecular photovoltaic devices, several additional features should be incorporated. These include multiple interfaces; finite spectral bandwidth, which will reduce V_{oc} compared to the monochromatic case; energetic heterogeneity, which leads to trapping of charge carriers in lower-energy levels and will reduce V_{oc}; Coulombic effects on excited states and transitions; intermediate states in charge separation, such as bound polaron pairs; bimolecular recombination between neighboring molecular systems; and heterogeneity in the molecular assembly, which may lead to shunt paths between the electrodes, reducing both fill factor and V_{oc}. The model presented here provides a basis to study such systems of more complex energetic and geometric structure, once appropriate parameters are known. In this respect a more complex, two-dimensional model has been developed recently to study the effect of morphology on the efficiency of donor-acceptor systems;[44] the qualitative effects of transfer rates and energetics in that model are compatible with the predictions of the simple model presented here.

V. CONCLUSIONS

In conclusion, we have presented a simple model of a molecular photovoltaic device based on a two-level, light absorbing system, connected to external electrodes by chains of charge transporting orbitals. Using detailed-balance arguments to describe photon absorption and emission, and nonadiabatic Marcus theory for electron transfer, we find simple mathematical expressions governing the steady-state current-voltage characteristics of such a system. This allows us to study the effect of intermolecular charge transfer on the power conversion efficiency without considering the effect of spectral sensitivity. We focus on several simple configurations which can be solved analytically or with simple numerical calculations. For perfect absorption and lossless charge transfer to the electrodes, monochromatic power conversion efficiencies of 70% are predicted. Slow charge transfer due to large energy steps at the electrodes leads to slow charge collection rates and degrades the fill factor, even though dark currents are low. Fast charge transfer leads to strong interfacial recombination, reduced V_{oc}, and a crossing in light and dark J-V curves. In this limit the open-circuit voltage is linked to the difference in acceptor and donor energy levels. Extended chains of acceptors and donors connecting the sensitizer to electrodes lead to degraded J-V curves, reminiscent of series resistance effects, if charge mobilities are low. Although the model is highly simplistic, all of these effects are observed in experimental systems. To increase the monochromatic power conversion efficiency above the 10–20 % currently achievable, charge-carrier mobilities should be improved, ohmic contacts should be used, and electron-transfer rates at the heterojunction should be optimized.

ACKNOWLEDGMENTS

The authors are grateful to James Durrant and Pablo Etchegoin for useful discussions, to Sandrine Heutz and Sachetan Tuladhar for discussions of unpublished experimental data and to the coauthors of Ref. 33 for permission to reproduce the data in that paper. J.N. is grateful to the EPSRC, J.K. to the Rank Prize Funds, and P.R. to the Association of Commonwealth Universities for financial support.

APPENDIX

In case (b) J_g is given by the solution to

$$J_g = q\rho d\left(G_s + G_0 - \frac{K_g}{x_c^2 - 1}\right)\left(\frac{x_c - 1}{x_c + 1}\right) \tag{A1}$$

and

$$qV = 2(\mu_a - \mu_0) = 2E_a - E_g - 2kT \ln x_a, \quad \text{(A2)}$$

where $x_a = 1/f_a - 1$, $x_c = 1/f_c - 1$, and

$$f_a = \frac{K_{ac} f_c - K_{av}\delta_{av}(1-f_c) - J_g/q\rho d}{(K_{ca} - K_{av}) f_c - (K_{av}\delta_{ca} - K_{av}\delta_{av})(1-f_c)} \quad \text{(A3)}$$

with $\delta_{ca} = e^{-(E_c - E_a)/kT}$ and $\delta_{av} = e^{-(E_a - E_v)/kT}$. Knowing f_a and f_c allows one to calculate J_{ca} and hence J_{av} and J, for x_c within the allowed range. The limits to x_c are determined by the constraints that the occupation function of the acceptor level, f_a, must be $\geqslant 0$, giving an upper limit to x_c, and $f_a \leqslant 1$, giving a lower limit to x_c. The limiting x_c values are the solutions to quadratic equations for each of the two limits.

In the limit of no intermolecular recombination, case (b) simplifies to Eq. (16) with x given by the positive root of

$$(G_s + G_0 + K_{ca}\delta_{ca} f_a)x^2 - [K_{ca}(1-f_a) - K_{ca} f_a \delta_{ca}]x - [G_s + G_0 + K_g + K_{ca}(1-f_a)] = 0 \quad \text{(A4)}$$

and V by $qV = 2E_a - E_g - 2kT \ln x_a = 2E_a - E_g - 2kT \ln(1/f_a - 1)$ as above. In this limit V_{oc} is identical to the detailed-balance limit in case (a).

*Electronic mail: jenny.nelson@imperial.ac.uk

[1] J. Kruger, R. Plass, M. Gratzel, and H.-J. Matthieu, Appl. Phys. Lett. **81**, 367 (2002).

[2] P. Peumans and S.R. Forrest, Appl. Phys. Lett. **79**, 126 (2001).

[3] C.J. Brabec, S.E. Shaheen, C. Winder, N.S. Sariciftci, and P. Denk, Appl. Phys. Lett. **80**, 1288 (2002).

[4] B.A. Gregg and M. Hanna, J. Appl. Phys. **93**, 3605 (2003).

[5] C.M. Ramsdale, J.A. Barker, A.C. Arias, J.D. MacKenzie, R.H. Friend, and N.C. Greenham, J. Appl. Phys. **92**, 4266 (2002).

[6] J.A. Barker, C.M. Ramsdale, and N.C. Greenham, Phys. Rev. B **67**, 075205 (2003).

[7] C.J. Brabec, A. Cravino, D. Meissner, N.S. Sariciftci, T. Fromherz, M.T. Rispens, L. Sanchez, and J.C. Hummelen, Adv. Funct. Mater. **11**, 374 (2001).

[8] P. Peumans, A. Yakimov, and S.R. Forrest, J. Appl. Phys. **93**, 1 (2003).

[9] T. Markvart, Prog. Quantum Electron. **24**, 107 (2000).

[10] A. de Vos, *Endoreversibe Thermodynamics of Solar Energy Conversion* (Oxford University Press, New York, 1992).

[11] K. Emery and M.A. Green, Prog. Photovoltaics **11**, 39 (2003).

[12] B. O'Regan and M. Gratzel, Nature (London) **353**, 737 (1991).

[13] P. Wurfel, J. Phys. C **15**, 3967 (1982).

[14] T. Trupke, P. Wurfel, I. Uhlendorf, and I. Lauermann, J. Phys. Chem. B **103**, 1905 (1999).

[15] R.A. Marcus, Rev. Mod. Phys. **65**, 599 (1993).

[16] W. Schmickler, *Interfacial Electrochemistry* (Oxford University Press, New York, 1996).

[17] C.J. Brabec, G. Zerza, G. Cerullo, S. De Silvestri, S. Luzzatti, J.C. Hummelen, and N.S. Sariciftci, Chem. Phys. Lett. **340**, 232 (2001).

[18] N.S. Sariciftci, L. Smilowitz, A.J. Heeger, and F. Wudl, Science **258**, 1474 (1992).

[19] Y. Tachibana, J.E. Moser, M. Gratzel, D.R. Klug, and J.R. Durrant, J. Phys. Chem. **100**, 20056 (1996).

[20] M. Gratzel, Nature (London) **414**, 338 (2001).

[21] J.J.M. Halls, C.A. Walsh, N.C. Greenham, E.A. Marseglia, R.H. Friend, S.C. Moratti, and A.B. Holmes, Nature (London) **376**, 498 (1995).

[22] R. Pacios and D.D.C. Bradley, Synth. Met. **127**, 261 (2002).

[23] A.C. Arango, L.R. Johnson, V.N. Bliznyuk, Z. Schlesinger, S.A. Carter, and H.-H. Hrhold, Adv. Mater. (Weinheim, Ger.) **12**, 1689 (2000).

[24] C.J. Brabec, N.S. Sariciftci, and J.C. Hummelen, Adv. Funct. Mater. **11**, 15 (2001).

[25] James Durrant (private communication).

[26] J.J.M. Halls, K. Pichler, R.H. Friend, S.C. Moratti, and A.B. Holmes, Appl. Phys. Lett. **68**, 3120 (1996).

[27] M. Granstrom, K. Petritsch, A.C. Arias, A. Lux, M.R. Andersson, and R.H. Friend, Nature (London) **395**, 257 (1998).

[28] A.F. Nogueira, M.A. De Paoli, I. Montanari, R. Monkhouse, J. Nelson, and J.R. Durrant, J. Phys. Chem. B **105**, 7517 (2001).

[29] J. Nelson and J. Kirkpatrick, Appl. Phys. A (to be published).

[30] J. Stephan, S. Schrader, and L. Brehmer, Synth. Met. **111-112**, 353 (2000).

[31] K. Takahashi, N. Kuraya, T. Yamaguchi, T. Komura, and K. Murata, Sol. Energy Mater. Sol. Cells **61**, 403 (2000).

[32] Sandrine Heutz (private communication).

[33] P. Ravirajan, S.A. Haque, D. Poplavskyy, J.R. Durrant, D.D.C. Bradley, and J. Nelson, J. Appl. Phys. (to be published).

[34] P. Ravirajan, S.A. Haque, D. Poplavskyy, J.R. Durrant, D.D.C. Bradley, and J. Nelson, Thin Solid Films (to be published).

[35] E.A. Katz, D. Faiman, S.M. Tuladhar, J.M. Kroon, M.M. Wienk, T. Fromherz, F. Padinger, C.J. Brabec, and N.S. Sariciftci, J. Appl. Phys. **90**, 5343 (2001).

[36] S. M. Tuladhar (private communication).

[37] I. Montanari, A.F. Nogueira, J. Nelson, and J.R. Durrant, C. Winder, M.A. Loi, N.S. Sariciftci, and C. Brabec, Appl. Phys. Lett. **81**, 3001 (2002).

[38] J. Kruger, R. Plass, L. Cevey, M. Piccirelli, M. Gratzel, and U. Bach, Appl. Phys. Lett. **79**, 2085 (2001).

[39] E. Palomares, J.N. Clifford, S.A. Haque, T. Lutz, and J.R. Durrant, J. Am. Chem. Soc. **125**, 475 (2003).

[40] Y. Liu, A. Hagfeldt, X.-R. Xiao, and S.-E. Lindquist, Sol. Energy Mater. Sol. Cells **55**, 267 (1998).

[41] S.A. Haque, T. Park, A.B. Holmes, and J.R. Durrant, ChemPhysChem **1**, 89 (2003).

[42] S.E. Shaheen, C.J. Brabec, N.S. Sariciftci, F. Padinger, T. Fromherz, and J.C. Hummelen, Appl. Phys. Lett. **78**, 841 (2001).

[43] Transient optical measurements show that the injection rate from Ru based dye into nanocrystalline TiO_2 in dye-senitized solar cells is reduced on addition of basic organic molecules such as pyridine, even though these additives increase the V_{oc} and efficiency of devices. E. Palomares (private communication).

[44] K.O. Sylvester-Hvid, S. Rettrup, and M.A. Ratner (unpublished).